Reconfigurable Intelligent Surface (RIS) Design for 5G n260 Frequency Band

Reza Yazdani
EMC Laboratory, Department of electrical engineering
Missouri university of science and technology
Rolla, Mo, USA
ryazdani@mst.edu

Manish Kizhakkeveettil Mathew
EMC Laboratory, Department of electrical engineering
Missouri university of science and technology
Rolla, Mo, USA

Zhekun Peng
EMC Laboratory, Department of electrical engineering
Missouri university of science and technology
Rolla, Mo, USA

DongHyun Kim
EMC Laboratory, Department of electrical engineering
Missouri university of science and technology
Rolla, Mo, USA

2023 IEEE Symposium on Electromagnetic Compatibility & Signal/Power Integrity (EMC+SIPI) | 979-8-3503-0976-8/23/$31.00 ©2023 IEEE | DOI: 10.1109/EMCSIPI50001.2023.10241407

***Abstract*—In this paper, a new low profile reconfigurable intelligent surface design with high resolution steering reflector and wide frequency band width is proposed at n260 frequency band, used for 5G new radio applications. The dynamic reflection phase and tunability is realized by integrating of varactor diode with each unit cell. This study presents design procedures, reflection simulation verifications, and the effects of important parameters on the performance of the proposed novel resonant unit cell. The proposed unit cell offers a dynamic reflection phase range of more than 270◦ at a wide frequency bandwidth. Simulation results of beam steering capability in horizontal plane at 38 GHz is presented to verify the design performance of the RIS.**

Keywords—unit cell, RIS, 5G, varactor diode

I. INTRODUCTION

Fifth generation (5G) wireless communication system is increasing popular research topic in academia and industry due to the rapid growth in mobile data usage and number of Internet of Things (IoT) in the market. To fulfill the user demands, the specifications of the 5G wireless network requires increase effectiveness and power than its previous generations [1]. To reach high bandwidth, the next generation of mobile communications is designed to work at millimeter-wave (mmWave) frequency or even at terahertz frequency [2], thus the attenuation issue in such high frequency bands will increase at the same distance, the signal quality degradation will be severe. The quality of service (QoS) can be easily deteriorated by simple obstacles such as wall, furniture, or a person between the transmitter and receiver [3-5].

Reconfigurable intelligent surface (RIS) is one of the promising technologies that can improve the attenuation issue [6,7]. By changing the phase, amplitude, frequency, or polarization of the incident EM wave RIS can adaptively reconfigure the wireless environment without active user input [8]. When there is not a direct line of sight between the transmitter and receiver due to obstacles between them or when the channel quality between the transmitter and receiver is too lossy the RIS can be applied to provide an alternative path or to enhance the quality, respectively. Therefore, the main objective of RIS is to deliberately and deterministically control the propagation environment to improve the signal quality at the receiver [9]. A dominant feature of RISs is, therefore, to provide a propagation path when no line of sight (LoS) exists due to their unique ability to be reconfigurable after their deployment in a wireless environment.

In comparison to other related technologies which are currently used in wireless networks, including MIMO relaying, beamforming, and backscatter communications, RISs are different. Major difference is that RIS do not need any active elements such as radio frequency (RF) chains to reflect, focus, steer, or scatter the incident EM wave, and they are passive elements. This characteristic makes an RIS substantially low cost with less mechanical and electrical complexity, and low power consumption compared to their counterparts such as phased array antenna or relay [4]. RIS includes hundreds of unit cells each of which are able to shape the incident wave and reflect it to the desired location or receiver. Therefore, unit cell plays an important role in the final RIS design. As RIS does not need analog-to-digital/digital-to-analog converters, and power amplifiers, and it is not affected by receiver noise. Consequently, they do not introduce any additional noise to the communication link [3]. RIS can work at a wide range of frequencies, and they have a full-band response. By applying controllable elements such as diodes the state of RIS can be changed, and one can steer the main beam of the reflected wave [10,12]. As shown in Fig. 1, simplicity and low profile make the RIS an easy structure to simply attached them to walls or ceilings of indoor environments to boost the signal quality (Fig. 1).

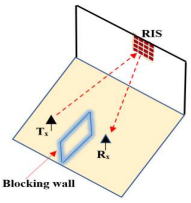

Fig. 1. Application scenario

II. UNIT CELL DESIGN

The single unit cell (or pixel) of the designed RIS is represented by a conducting square patch (made of copper) placed on a low loss grounded dielectric substrate ROGERS RT5880 ($\varepsilon = 2.2$, $\tan(\delta) = 0.0009$ @ 10 GHz). The upper patch

receives and radiates energy, while the ground plane suppresses the back radiation. The top and front view of the proposed unit cell is shown in Fig. 2. The top copper layer has two vertical strips which are connected to horizontal conductor pads designed as per the varactor layout. From Fig. 2(a) it can be seen that slots were used on each vertical strips to get the desired frequency range. The varactor used in this unit cell is the MAVR-011020-1411 model manufactured by MACOM which provides extremely low capacitance. [13]. The left strip is shorted by via to the metal ground. Since the varactor is placed in between the unit cells, it will provide a variable capacitance C_d to the unit cell. This varactor model has a dynamic capacitance range of C_{max}= 0.22 pF and C_{min} =0.033pF for a reverse bias voltage of 0-15 V, respectively.

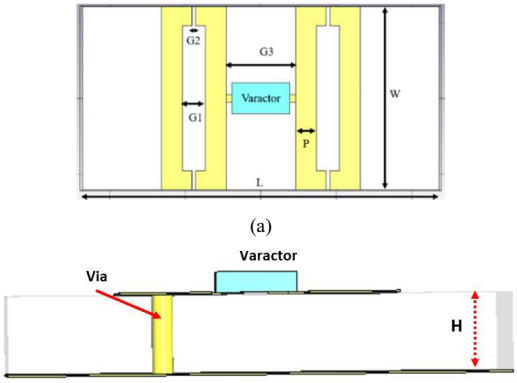

Fig. 2. Proposed unit cell, (a)top view, (b) side view

The proposed unit cell is simulated using the TEM Floquet port with CST microwave studio simulation software, and its parameter values (see Table 1) are obtained after optimization. The unit cell is designed to provide the patch resonance frequency (f_0)to be approximately around 38 GHz. By using single layer and one diode in each unit cell in compare with [14] which has two substrate layer and two diodes for each unit cell, the proposed method is able to introduce a cost-effective and low profile structure for the final RIS fabrication.

It is worth mentioning that the internal inductance (L_{int}) and capacitance (C_{int}) of the unit cell is determined by the factors like unit cell geometry, tunable element property, materials, and the PCB manufacturing process. The unit cell resonates at a frequency given by,

$$f_{res} = \frac{1}{2\pi\sqrt{LC}} \quad (1)$$

Here, a varactor is considered as the tunable element to change the capacitance of the unit cell, thereby varying the resonance frequency. The $C_{int}$and $L_{int}$are proportional to the surface area of the unit cell and the thickness of the substrate, respectively. So, the total capacitance and inductance of the unit cell will be C= C_{int}+ C_d and L=L_{int}, where C_d is the variable capacitance provided by the varactor diode for different dc bias voltages. It can be inferred that a smaller LC product yield a higher resonance frequency. It is difficult to vary the inductance of the unit cell. The advantage of choosing capacitance as the tunable element is that the capacitance is directly proportional to the Q factor and unit cell absorption.

TABLE. 1. UNIT CELL PARAMETERS

Parameter	Description	Value[mm]
L	*Unit Length*	4.7
W	*Unit Width*	2.4
P	*Strip Width*	0.3
G_1	*Gap within the strips*	0.2
G2	*The smaller gap within the strips*	0.05
G3	Distance between inner strips	0.91
H	Height of dielectric substrate	0.73

A. Fullwave Simulation Results:

The reflection coefficient of the unit cell for a normal incidence of a wave as a function of frequency was simulated by varying the capacitance of the varactor using a linear parametric sweep from C_{min} to C_{max}. It is clear from Fig. 3 that the unit cell is resonating in the frequency range from 31.5 GHz to 39.5 GHz for the maximum and minimum capacitance provided by the varactor diodes while they are biased by a 0V and 15 V respectively. This provided a dynamic reflection phase range of 270◦. As shown in Fig. 3(a) this parameter is highly related to the capacitance range of the varactor diode, and one can improve the dynamic reflection phase of the unit cell by using a diode with larger capacitance range.

The via was used for the DC bias for the varactor diode. The standard via diameter for manufacturing is 0.25 mm–0.30 mm, which had no effect on the unit cell's performance.

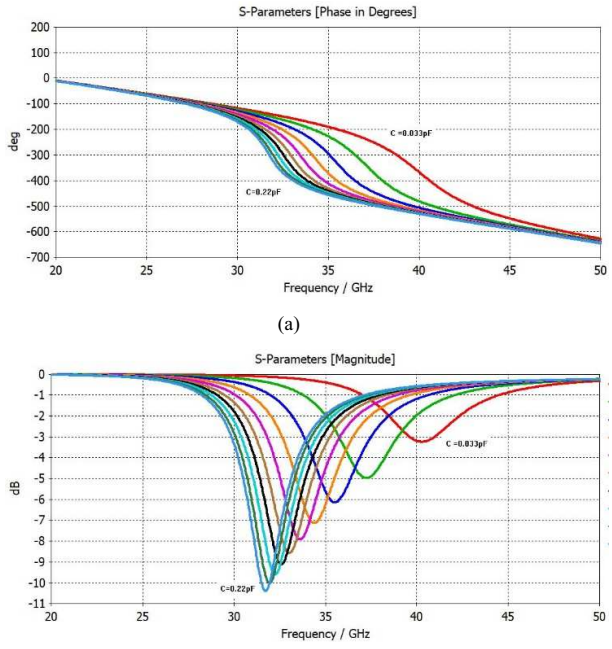

Fig. 3. Reflection coefficient simulation of the unit cell (a) reflection phase, (b) reflection magnitude

B. Parameter Analysis:

To analyze the different tunable parameters' effect on the reflection coefficient, a parametric study is done in the CST microwave studio. During this study, the capacitance value was fixed to 0.033 pF and the effect of the important parameters that have considerably effect on the performance of the unit cell including width, substrate height, gaps G_1 and G_2 are studied.

As shown in Fig. 4 by increasing *W* the resonant frequency decreases from 38.5GHz to 37.5GHz.

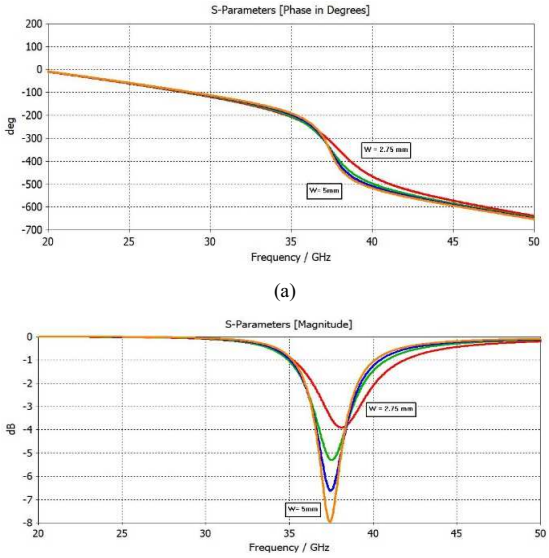

(a)

(b)

Fig. 4. Effect of *W* on the reflection coefficient. (a) reflection phase, (b) reflection magnitude

Changing the height of the substrate has negligible effect on the resonant frequency, but as it can be seen from Fig. 5(a) increasing the height to 1 mm can significantly decrease the loss of the incident wave. Therefore, to reach to the minimum loss the optimum value for *H* is 1mm.

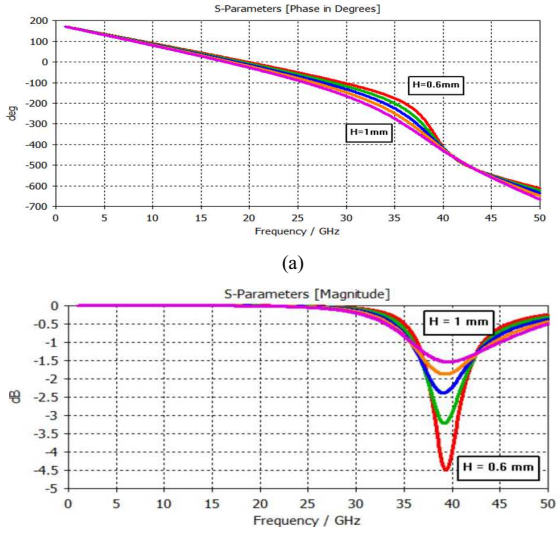

(a)

(b)

Fig. 5. Effect of *H* on the reflection coefficient. (a) reflection phase, (b) reflection magnitude

In next step the gap inside the vertical strips was swept from 0.1mm to 0.5 mm. From Fig. 6 it is clear that by decreasing this gap from 0.5mm to 0.1 mm we are able to decrease the loss for about 0.5dB.

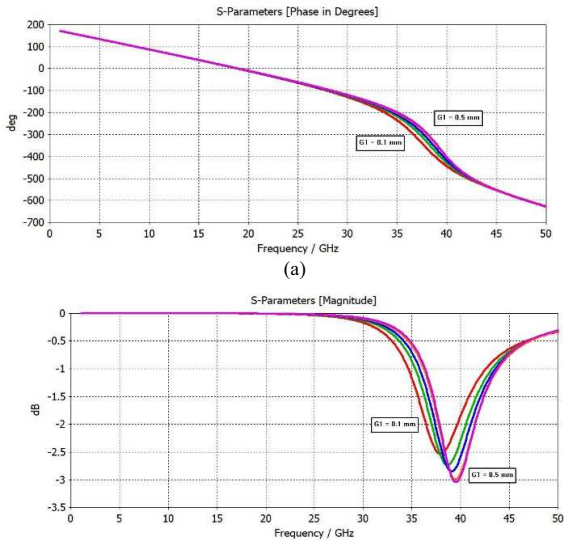

(a)

(b)

Fig. 6. Effect of G_1 on the reflection coefficient. (a) reflection phase, (b) reflection magnitude

As it can be seen from Fig. 7 the smaller gap within the strip G_2 can change the resonant frequency. Changing this parameter from 0.01 mm to 0.1 mm can change the resonant frequency from 36 to 40.5GHz.

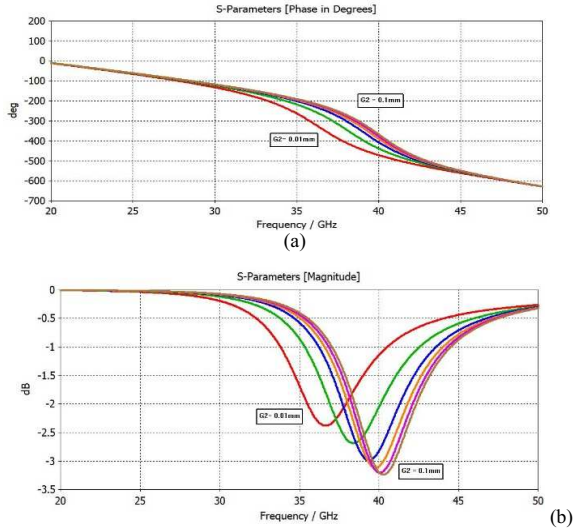

(a)

(b)

Fig. 7. Effect of *G2* on the reflection coefficient. (a) reflection phase, (b) reflection magnitude

III. RIS ARRAY DESIGN:

An array with 20 rows and 16 columns, having a total of 320 unit cells is designed to realize the RIS. The total dimension of the final RIS is 48×75.2 mm.

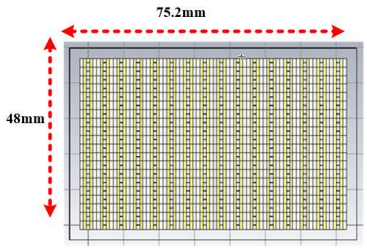

Fig. 8. The RIS of the proposed unit cell

To operate, a RIS is required to modify the phase of the reflected wave in comparison to the incident wave and not to dissipate all the incident power. The steering angle θ is achieved by the gradual accumulation of phase difference $\Delta\varphi$ between each column of the RIS array. The beam steering angle θ is related to $\Delta\varphi$, operating wavelength λ, and array constant ΔX [14].

$$\theta = sin^{-1}\left(\frac{\lambda\Delta\varphi}{360.\Delta x}\right) \quad (2)$$

Where ΔX is the length of the unit cell.

A phase calibration curve of the reflection phase to the varactor capacitance at 34 GHz is obtained by post-processing the reflection phase to frequency swept through the maximum and minimum varactor capacitance values (see Fig. 9).

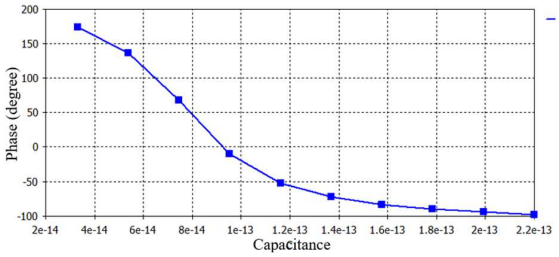

Fig. 9. Simulation results of the varactor diode capacitance versus phase variation

Therefore, the appropriate dc bias voltage that needs to be provided to each column to achieve a required phase difference $\Delta\varphi$ can be extracted from the phase calibration curve. Therefore, each column of the RIS with specific applied voltage become capable of re-radiating an electromagnetic field having a specific phase state. Hence, the desired electronic phase control capability is realized without using conventional phase shifters. To show the beam steering capability the RIS structure is simulated in the CST microwave studio. As can be seen from Fig. 10. the main lobe radiation pattern of the proposed RIS structure is properly steered in the horizontal plane toward the user side.

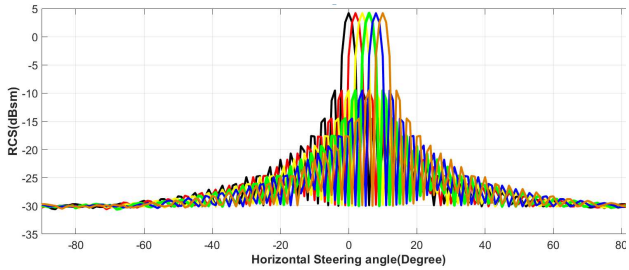

Fig. 10. Beam steering capability of the proposed RIS at 38 GHz

IV. Conclusion

In this study, a novel unit cell is introduced to use in the RIS design, and it can fully cover the n260 frequency band, which is one of the promising bands for 5G communication applications. In compare with the previous works by decreasing the number of layers and diodes the proposed unit cell introduced a low profile and cost-effective solution for the RIS design. A varactor diode with a variable capacitance is used to realize a 270◦ dynamic reflection phase. The simulation results successfully demonstrate the high-efficiency beamforming capability and electronic phase shifting.

References

[1] Tang, Wankai, Ming Zheng Chen, Xiangyu Chen, Jun Yan Dai, Yu Han, Marco Di Renzo, Yong Zeng, Shi Jin, Qiang Cheng, and Tie Jun Cui. "Wireless communications with reconfigurable intelligent surface: Path loss modeling and experimental measurement." IEEE Transactions on Wireless Communications 20, no. 1 (2020): 421-439.

[2] Rappaport, T.S., et al., Millimeter Wave Mobile Communications for 5G Cellular: It Will Work! IEEE Access, 2013. 1: p. 335-349.

[3] Basar, Ertugrul, Marco Di Renzo, Julien De Rosny, Merouane Debbah, Mohamed-Slim Alouini, and Rui Zhang. "Wireless communications through reconfigurable intelligent surfaces." IEEE access 7 (2019): 116753-116773.

[4] Amri, Muhammad Miftahul, Nguyen Minh Tran, and Kae Won Choi. "Reconfigurable intelligent surface-aided wireless communications: adaptive beamforming and experimental validations." IEEE Access 9 (2021): 147442-147457.

[5] Cho, Kun Woo, Mohammad H. Mazaheri, Jeremy Gummeson, Omid Abari, and Kyle Jamieson. "mmWall: A reconfigurable metamaterial surface for mmWave networks." In Proceedings of the 22nd International Workshop on Mobile Computing Systems and Applications, pp. 119-125. 2021.

[6] Kisseleff, Steven, Wallace A. Martins, Hayder Al-Hraishawi, Symeon Chatzinotas, and Björn Ottersten. "Reconfigurable intelligent surfaces for smart cities: Research challenges and opportunities." IEEE Open Journal of the Communications Society 1 (2020): 1781-1797.

[7] Yildirim, Ibrahim, Ali Uyrus, and Ertugrul Basar. "Modeling and analysis of reconfigurable intelligent surfaces for indoor and outdoor applications in future wireless networks." IEEE transactions on communications 69, no. 2 (2020): 1290-1301.

[8] Araghi, Ali, Mohsen Khalily, Mahmood Safaei, Amirmasood Bagheri, Vikrant Singh, Fan Wang, and Rahim Tafazolli. "Reconfigurable intelligent surface (ris) in the sub-6 ghz band: Design, implementation, and real-world demonstration." IEEE Access 10 (2022): 2646-2655.

[9] Dai, Linglong, Bichai Wang, Min Wang, Xue Yang, Jingbo Tan, Shuangkaisheng Bi, Shenheng Xu et al. "Reconfigurable intelligent surface-based wireless communications: Antenna design, prototyping, and experimental results." IEEE access 8 (2020): 45913-45923.

[10] Di Renzo, Marco, Alessio Zappone, Merouane Debbah, Mohamed-Slim Alouini, Chau Yuen, Julien De Rosny, and Sergei Tretyakov. "Smart radio environments empowered by reconfigurable intelligent surfaces: How it works, state of research, and the road ahead." IEEE journal on selected areas in communications 38, no. 11 (2020): 2450-2525.

[11] Rahamim, Efi, David Rotshild, and Amir Abramovich. "Performance Enhancement of Reconfigurable Metamaterial Reflector Antenna by Decreasing the Absorption of the Reflected Beam." Applied Sciences 11, no. 19 (2021): 8999.

[12] Gros, Jean-Baptiste, Vladislav Popov, Mikhail A. Odit, Vladimir Lenets, and Geoffroy Lerosey. "A reconfigurable intelligent surface at mmWave based on a binary phase tunable metasurface." IEEE Open Journal of the Communications Society 2 (2021): 1055-1064.

[13] MACOM AVR-011020-1411, Solderable GaAs Constant Gamma Flip-chip Varactor Diode. Available online: https://cdn.macom.com/datasheets/MAVR-011020-1141.pdf (accessed on 11 June 2020).

[14] Rotshild, David, Efraim Rahamim, and Amir Abramovich. "Innovative reconfigurable metasurface 2-D beam-steerable reflector for 5G wireless communication." *Electronics* 9.8 (2020): 1191.